AFCRL-65-53

AN EXPERIMENTAL STUDY OF PLASMA SHEATH EFFECTS ON ANTENNAS

BY

GEORGE TYRAS
PETER C. BARGELIOTES
JOHN M. HAMM
ROBERT R. SCHELL

THE UNIVERSITY OF ARIZONA
COLLEGE OF ENGINEERING
ENGINEERING RESEARCH LABORATORIES
TUCSON, ARIZONA

CONTRACT NO. AF 19(628)-3834
PROJECT 4642
TASK 464202

SCIENTIFIC REPORT NO 1

DECEMBER 1964

PREPARED FOR

AIR FORCE CAMBRIDGE RESEARCH LABORATORIES
OFFICE OF AEROSPACE RESEARCH
UNITED STATES AIR FORCE
BEDFORD, MASSACHUSETTS

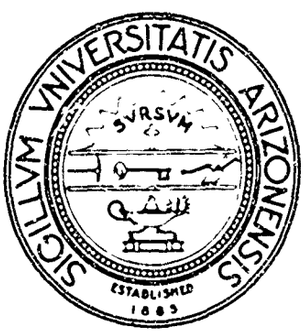

AFCRL- 65-53

AN EXPERIMENTAL STUDY OF PLASMA SHEATH EFFECTS ON ANTENNAS

by

George Tyras
Peter C. Bargeliotes
John M. Hamm
Robert R. Schell

The University of Arizona
College of Engineering
Engineering Research Laboratories
Tucson, Arizona

Contract No. AF 19(628)-3834
Project 4642
Task 464202

Scientific Report No. 1

December 1964

PREPARED FOR

Air Force Cambridge Research Laboratories
Office of Aerospace Research
United States Air Force
Bedford, Massachusetts

Requests for additional copies by agencies of the Department of Defense, their contractors, and other Government agencies should be directed to:

Defense Documentation Center (DDC)
Cameron Station
Alexandria, Virginia 22314

Department of Defense contractors must be established for DDC services or have their "need-to-know" certified by the cognizant military agency of their project or contract.

All other persons and organizations should apply to the:

U. S. Department of Commerce
Office of Technical Services
Washington, D. C. 20230

TABLE OF CONTENTS

TABLE OF FIGURES

ABSTRACT

A plasma simulation technique has been developed which can be used to study the effects of homogeneous or inhomogeneous plasma sheath on the radiation pattern deterioration and input impedance of microwave antennas. A tank has been designed and constructed for use in the simulation technique which can reproduce by means of real dielectric materials the dielectric constant encountered in plasma covered antenna research.

The radiation patterns and the input impedances of an annular slot and a thin and long rectangular slot have been successfully measured in the presence of a simulated loss-less, homogeneous and isotropic plasma layer of varied thickness. Comparison with the available theoretical data indicates a generally good agreement, although some differences exist. In the case of the radiation patterns these differences are attributed to the finite distance between the radiator and the receiving antenna on one hand and the inherent inaccuracy of the saddle point method of integration in certain regions on the other hand.

1. Introduction

Recent aerospace achievements have motivated a great number of investigations into wave propagation through plasma sheaths. Most of these investigations are of theoretical nature and they use an infinite, isotropic, homogeneous, and uniform plasma slab as a model for reentry environment of a radiating system. In order to experimentally verify the theoretical work and to obtain the results for more realistic radiating system and plasma sheath configurations, a laboratory simulation of a plasma sheath is very desirable. The most recent simulation attempts make use of artificial dielectrics, especially rodded media [Rotman, 1962; Golden and Smith, 1964; Golden, 1964]. These attempts are based on the fact that rodded media have refractive indices less than unity under certain conditions [Brown, 1953].

The results of these experiments generally match the theory. Certain important points, however, were not found to coincide with the theory. For example, the sharp peaks at the critical angle, $\sin \theta_c = n$, were not found as expected when an E plane slot antenna was used [Golden, 1964] . Such discrepancies are possibly due to "higher-order reflections" from the rodded media which result with increasing oblique incidence [Brown, 1953] .

It is the purpose of this report to introduce another method of simulating the plasma sheath. This method will be seen to provide an exact determination of the simulated plasma parameters and a laboratory geometry for which it is a simple matter to accurately adjust and vary the slab thickness.

The simulation method, to be described in detail in a later section, permitted the recording of the field patterns in the region outside of the plasma sheath. The radiators used were an annular slot and a rectangular slot in a ground plane. Field strength and admittance measurements were made for each antenna with various slab thicknesses. The comparison of the experimental results with theory determines the feasibility of this method as a valid plasma

sheath simulation technique. This feasibility has been established for a lossless plasma and in the case of thicker plasma slabs it is limited only by the size of the simulation tank used.

2. Theoretical Background

2.1 Annular Slot Antenna

An annular slot cut in an infinitely conducting plane and covered by a thin layer of lossless isotropic and homogeneous plasma will be considered first. The geometry of the problem is shown in Figure 1.

The slot is assumed to be of narrow width with a mean radius "b". A constant voltage "V" is assumed to be present across the slot. The horizontal plane $z = a$ coincides with the interface of the homogeneous plasma layer and the surrounding medium. For convenience, reference will be given to the surrounding medium (1) and plasma medium (2) with relative dielectric constants ϵ_1 and ϵ_2, respectively.

It is clearly seen from the symmetry of the problem that there is no variation in the ϕ-coordinate, i.e., $\frac{\partial}{\partial \phi} = 0$, and only the H_ϕ component of the magnetic field exists. Furthermore, it is noted that the electric field at the aperture is

$$E_\rho = - V\delta(\rho - b)\delta(z) \tag{1}$$

Assuming the $e^{-i\omega t}$ time-dependence and suppressing it throughout, the electric field components are given by

$$E_\rho = \frac{1}{i\omega\epsilon_o\epsilon} \frac{\partial H_\phi}{\partial z} \tag{2a}$$

and

$$E_z = - \frac{1}{i\omega\epsilon_o\epsilon} \frac{1}{\rho} \frac{\partial}{\partial \rho} (\rho H_\phi) \tag{2b}$$

where H_ϕ satisfies the equation

$$\frac{\partial}{\partial \rho}\left[\frac{1}{\rho}\frac{\partial}{\partial \rho}(\rho H_\phi)\right] + \frac{\partial^2 H_\phi}{\partial z^2} + k^2 H_\phi = \begin{cases} -V\delta(\rho-b)\delta(z), & 0 < z < a \\ 0, & z > a . \end{cases} \tag{3}$$

The solution of (3) has been found to be [Tyras, 1962]

$$H_{\phi 1} = \frac{iVb\omega\epsilon_o n^2}{2} \int_{-\infty}^{+\infty} \frac{e^{-\gamma_1(z-a)} J_1(\lambda b) H_1^{(1)}(\lambda\rho) \cdot \lambda d\lambda}{[\gamma_2 \sinh(\gamma_2 a) + n^2 \gamma_1 \cosh(\gamma_2 a)]} \tag{4a}$$

$$H_{\phi 2} = \frac{iVb\omega\epsilon_o n^2}{2} \int_{-\infty}^{+\infty} \frac{[\gamma_2 \cosh\ \gamma_2(a-z) + n^2\gamma_1 \sinh\ \gamma_2(a-z)]}{\gamma_2[\gamma_2 \sinh(\gamma_2 a) + n^2\gamma_1 \cosh(\gamma_2 a)]} \quad J_1(\lambda b) H_1^{(1)}(\lambda\rho)\lambda d\lambda \tag{4b}$$

where

$$\gamma_i = \sqrt{\lambda^2 - k_i^2} \tag{4c}$$

$$k_i = 2\pi/\lambda_i \quad , \quad n^2 = \epsilon_2/\epsilon_1 \tag{4d}$$

Changing to spherical coordinates in the configuration space and taking $\lambda = k_1 \sin\beta$ in the transform space, (4a) is changed into a contour integral in the complex β-plane. The evaluation of the contour integral by the saddle point method gives the far-zone field

$$H_{\phi 1} = \frac{Y_1\ V\ k_1\ n^2\ b\ J_1(k_1 b \sin\theta)\ \cos\theta}{\sqrt{n^2 - \sin^2\theta}\ \sin(k_1 a \sqrt{n^2 - \sin^2\theta}\ ) + in^2 \cos\theta \cos(k_1 a \sqrt{n^2 - \sin^2\theta}\ )}$$

$$\cdot \frac{e^{i[k_1 r - \pi/4]}}{r} \tag{5}$$

where $Y_1 = \sqrt{\epsilon_o\epsilon_1/\mu_o}$ is the admittance of the surrounding medium. The far-zone electric field has the single component

$$E_{\theta 1} = Z_1\ H_{\phi 1} \tag{6}$$

where $Z_1 Y_1 = 1$. It is clear that (5) is valid for real as well as complex values of the plasma index of refraction, n .

The expression for the far-zone electric field has been programmed for the computer [Tyras, 1962] for different combinations of frequency and plasma thickness and the results are shown in Figure 2. The apparent feature that is common to all of these radiation patterns is the sharp attenuation for all angles larger than the critical angle. This fact is well explained from the consideration of geometric optics. Moreover, it is also evident that with the increasing electrical thickness of the plasma layer, progressively more ripples appear in the radiation pattern.

Equation (5) gives the complete solution of the fields in the radiation zone. However, "leaky wave" poles, poles arising from the singularities of the contour integral and located in the improper Riemann sheet, may significantly affect the near and intermediate zones. These "leaky waves" exhibit a radial attenuation and their effect on the radiation field diminishes even when strongly excited. An extensive treatment of complex poles is given by Tamir and Oliner [1962].

2.2 Rectangular Slot Antenna

The second kind of antenna considered is a thin rectangular slot in an infinite ground plane clad with plasma. The geometry of the problem is shown in Figure 1. Assuming that in the aperture there is a single component of the magnetic field, H_x , then it follows that the electric fields will be given by

$$E_y = \frac{i}{\omega \epsilon_o \epsilon} \frac{\partial H_x}{\partial z} \tag{7a}$$

and

$$E_z = \frac{-i}{\omega \epsilon_o \epsilon} \frac{\partial H_x}{\partial y} \quad . \tag{7b}$$

The solution can be formulated in a straightforward manner using Fourier transforms [Knop and Cohn, 1964] . One obtains

$$H_{x1} = \frac{\omega\epsilon_o n^2}{4\pi^2} \iint_{ap.} F_y(\xi,\eta)d\xi d\eta$$

$$\cdot \int_{-\infty}^{\infty}\int \frac{e^{i[\alpha_1(x-\xi)+\alpha_2(y-\eta)+s_1(z-a)]}}{n^2 s_1 \cos(s_2 a) - is_2 \sin(s_2 a)} \, d\alpha_1 d\alpha_2 \qquad (8)$$

for the air region and

$$H_{x2} = \frac{\omega\epsilon_o n^2}{4\pi^2} \iint_{ap.} F_y(\xi,\eta)d\xi d\eta$$

$$\cdot \int_{-\infty}^{\infty}\int \frac{in^2 s_1 \sin(s_2(z-a)) + s_2\cos(s_2(z-a))}{s_2(n^2 s_1\cos(s_2 a) - is_2\sin(s_2 a))} \; e^{i[\alpha_1 x-\xi)+\alpha_2(y-\eta)]} \, d\alpha_1 d\alpha_2 \qquad (9)$$

for the plasma region, where

$$s_i = \sqrt{k_i^2 - (\alpha_1^2 + \alpha_2^2)} \qquad (10)$$

$$k_i = 2\pi/\lambda_i$$

and $F_y(\xi,\eta)$ is the y-th component of the electric field in the aperture which is assumed to be known.

For the particular case at hand when the slot is narrow and very long one can assume the excitation of the form

$$F_y(\xi,\eta) = -V\delta(\eta) \tag{10}$$

where V is the voltage across the slot. Substituting (10) into (8) and using the saddle point method of integration, one obtains for the radiation field

$$H_{xo} = \frac{-\omega\epsilon_o n^2 V}{\sqrt{2\pi}} \cdot G(\theta) \frac{e^{i(k_o\rho-\pi/4)}}{\sqrt{k_o\rho}} \tag{11a}$$

where $G(\theta)$ is the form-factor given by

$$G(\theta) = \frac{\cos\theta}{n^2\cos\theta\cos(k_o a\sqrt{n^2-\sin^2\theta}) - i\sqrt{n^2-\sin^2\theta}\sin(k_o a\sqrt{n^2-\sin^2\theta})} . \tag{11b}$$

The expressions in (11) have been derived earlier by Newstein and Lurye [1956], Omura [1962] and Tamir and Oliner [1962]. Omura's report contains a considerable number of numerical results to which we shall later have the occasion to refer to for comparison with our experimental results. The work of Tamir and Oliner is devoted to interpretation of the results in terms of "leaky waves".

Both the numerical results of Omura [1962] and the "leaky wave" analysis of Tamir and Oliner [1962], as well as the simple consideration of geometric optics, predict that the radiation pattern will have peaks in the neighborhood of the critical angles. Moreover, as the thickness of the layer increases, progressively more minor peaks appear in the radiation pattern while the major lobes are still found in the vicinity of the critical angles [Tamir and Oliner, 1962] .

3. The Experimental System and Results

3.1 The Simulation Technique

Plasmas are characterized by a dielectric tensor which reduces to a complex scalar in the absence of external magnetostatic fields. Furthermore, the real part of the plasma dielectric constant is less than unity, namely, $\epsilon_p/\epsilon_a < 1$ where ϵ_p is the plasma dielectric constant and ϵ_a is the dielectric constant of free space. If, however, $\epsilon_p/\epsilon_a = \epsilon_{ps}/\epsilon_{as} < 1$ where the subscripts "ps" and "as" denote plasma simulation and air simulation, respectively, it is seen that a simulated plasma environment depends on the ratio of the dielectric constants and not on their absolute values. Thus an artificial plasma environment can be created by covering a radiator or a scatterer under investigation with a medium having a dielectric constant less than that of the free space simulator.

A major requirement of the free space simulator is that it be in the liquid form to allow movement of measuring equipment through it. Furthermore, it should have a low loss tangent to minimize signal attenuation in the medium. The plasma sheath simulator can be any foamy material with $\epsilon_r \sim 1$ or simply air itself. Such a combination of dielectric materials will simulate a plasma with $0 < \epsilon_p < 1$.

With such a simulation technique, the plasma parameters can be scaled and properly defined. Consider the annular slot as an example. The far zone electric field of the annular slot covered with the dielectric layer can be expressed from (5) as

$$E_o = \frac{bVk_o n^2 J_1(k_o b \sin\theta) \cos\theta \, e^{i(k_o r - \pi/4)} \cdot r^{-1}}{\sqrt{n^2 - \sin^2\theta}\, \sin(k_o a\sqrt{n^2-\sin^2\theta}) + in^2\cos\theta\cos(k_o a\sqrt{n^2-\sin^2\theta})} \tag{12}$$

where $n^2 = 1 - (\omega_p/\omega)^2$, "a" is the thickness of the dielectric layer, and "b" is the mean radius of the slot. If, however, the air is replaced by another dielectric medium, as in the proposed simulation technique, the far-zone field takes on the form

$$E_s = \frac{b_s V k_s n_s^2 J_1(k_s b_s \sin\theta) \cos\theta \, e^{i(k_s r - \pi/4)} \cdot r^{-1}}{\sqrt{n_s^2 - \sin^2\theta}\sin(k_s a_s\sqrt{n^2-\sin^2\theta}) + in_s^2\cos\theta\cos(k_s a_s\sqrt{n_s^2 - \sin^2\theta})} \tag{13}$$

where the subscript "s" denotes the equivalent simulation problem. The ratio E_s/E_o can be made constant by requiring that

$$\begin{aligned} n_s &= n \\ k_s a_s &= k_o a \\ k_s b_s &= k_o b \end{aligned} \tag{14}$$

and consequently defines the scaled plasma parameters.

The results of equation (14) can also be obtained directly from Maxwell's equations [Stratton, 1941]. It suffices to require that the two ratios remain invariant

$$c_1 = \mu\epsilon \left(\frac{\ell}{\tau}\right)^2$$

$$c_2 = \mu\sigma \frac{\ell^2}{\tau}$$

where τ is the characteristic period and ℓ denotes length. In the present case we are dealing with lossless dielectrics hence only c_1 need to be considered. Now the invariance of c_1 requires

$$\mu_s\epsilon_s\ell_s^2\omega_s^2 = \mu\epsilon\ell^2\omega^2$$

which leads directly to the latter two expressions of (14). Moreover, it is to be noted that if the dielectric permittivities are scaled by the same factor, say c_1 , then this factor must apply to all regions of space. Thus, if ϵ_1 refers to the plasma layer and ϵ_2 to the outer region then it follows that

$$c = \frac{\epsilon_1}{\epsilon_{1s}} = \frac{\epsilon_2}{\epsilon_{2s}}$$

and consequently

$$\frac{\epsilon_1}{\epsilon_2} = \frac{\epsilon_{1s}}{\epsilon_{2s}}$$

which is equivalent to first expression of (14).

The study of a table of dielectric materials [Von Hippel, 1958] at 10 Gc has revealed that the requirements of the free space simulating medium, i.e., low loss-tangent, non-corrosiveness, and stability are

satisfactorily met by Aroclor 1232 (Monsanto Chemical). The combination of air and Aroclor 1232 ($\epsilon_r = 2.78$ and $\tan \delta = 0.008$) will result in an $n_s = 0.60$ corresponding to an electron density per cubic centimeter $N = 7.83 \times 10^9 f_o^2$ where f_o is the actual antenna operating frequency in Gc. With the simulating frequency $f_s = 10$ G_c, air layer $a_s = 2.9$ cm, slot mean radius $b_s = 0.675$ cm and the simulating tank containing Aroclor 1232, it follows that $a/\lambda_o = 1.612$ and $b/\lambda_o = 0.375$. As a consequence of the scaling defined in (14) and since the plasma's index of refraction is a function of the wave frequency, the plasma environment that can be represented by this system will depend on the wave frequency chosen. Table I shows typical physical conditions of plasma sheath antenna environment that can be simulated with the Aroclor 1232 as free space and air as the plasma layer dielectric.

TABLE I

PLASMA SHEATH ANTENNA ENVIRONMENT REPRESENTABLE BY THE SYSTEM

f_o(Gc)	N(elect./cm^3	a(cm)	b(cm)
3	7.02×10^{10}	16.1	3.75
6	2.80×10^{11}	8.1	1.88
9	6.32×10^{11}	5.4	1.25
12	1.13×10^{12}	4.0	0.94
15	1.75×10^{12}	3.23	0.75

A semicylindrical tank of 22 inches inside radius and 24 inches high, as shown in Figure 3, was designed and subsequently built to the design specifications by the Paramount Plastic Fabricators of Downey, California. The wall material is plexiglass, $\epsilon_r = 2.59$. The flat wall of the tank is made of 1 inch plexiglass plate and the curved wall of 0.25 inch plexiglass. The tank holds 78 gallons of Aroclor 1232 oil, $\epsilon_r = 2.78$. At the operating frequency of 10 Gc, the tank allows a separation of the transmitting and the receiving antennas by at least 28 wavelengths.

Since the relative dielectric constants of the tank material and the oil are so close in value, the interface between them has negligible effect on the wave propagation. The reflections from the curved plexiglass-air interface were successfully reduced to a desirable level by placing high performance microwave absorber against the outside wall of the tank.

A ground plane was constructed using 0.312-inch thick aluminum plate mounted on 0.75-inch thick plywood. A 2-inch diameter hole was bored in the center of the plate and then counter-bored to 2.5-inch diameter. The counter-bored opening was accurately fitted with a separate machined piece which contained the annular slot antenna.

With the simulation tank located on top of a stationary bench, the ground plane could be situated conveniently at any distance in back of the simulation tank thus allowing the simulation of the plasma sheath of arbitrary thickness. The ground plane was mounted in the vertical plane atop a wooden cart equipped with rollers for ease of movement. The gap between the ground plane and the simulation tank was adjusted to the desired dimension by means of spacers and clamps to avoid accidental movement. The effects of the finite dimensions of both the ground plane and the simulated plasma layer were further aleviated by placing high performance microwave absorber around the finite boundaries of the simulated plasma layer. The absorber in this position acts as a matched termination of the plasma layer edges.

In the early simulation attempt, the ground plane was situated inside the simulation tank and a sealed styrofoam layer was used for the simulation of the plasma. However, this arrangement proved inadequate because both the styrofoam and the ground plane had to be rather small in size thus producing considerable open-ended waveguide radiation. Difficulties were also encountered in the sealing of the styrofoam sandwich.

The pick-up antenna consisted of a half-wave electric dipole on the end of a RG58A/U coaxial cable. The definition of the plane of the dipole was achieved by embedding the dipole in a plexiglass strip while its feeding cable was taken out of the tank along an L-bracket also made of plexiglass. The L-bracket was rigidly connected to a vertical shaft, the axis of which coincided with the center of the aperture in the ground plane. This type of arrangement allowed approximately $\pm 70^{\circ}$ coverage in the ψ direction for the largest simulated plasma layer of 2-inches in accordance with the slot coordinates as shown in Figure 1.

The output of the signal source was optimized at the operating frequency to maximize the sensitivity of the system and frequency stabilization was maintained during the measurements. The signal generator power was supplied by the Varian X-13 tube at 10 Gc. Frequency stabilization was achieved through the Dymec 2650A oscillator synchronizer. A Varian V-262 klystron was utilized as the local oscillator and it was operated at 9.970 Gc. Submersion of the tube in an oil bath assured the required frequency stability. The local oscillator was modulated with 1000 cps square wave. The signals from the pick-up dipole and the local oscillator were fed into the balanced mixer-preamplifier unit producing a 30 mc output which was subsequently fed into the high gain IF amplifier for further amplification. The 1000 cps square wave provided satisfactory modulation of the microwave signal so that an audio amplifier could be used with a crystal or a bolometer for detection, aiding in the calibration of the receiver. The receiver output was fed into the Antlab 1966 antenna pattern recorder which is equipped with a selective filter amplifier with 1000 cps center frequency and 4, 20, and 50 cycle bandwidths which feeds the pen system having linear, logarithmic, and square root modes.

The availability of theoretical radiation patterns of an annular slot [Tyras, 1962] and a thin, long rectangular slot [Omura, 1962] motivated the experimental investigation of these two types of radiators. An annular slot was constructed using brass stock because of the ease for precision machining. Since an annular slot of such narrow width has a very small impedance, a matching transformer was necessary to match the slot impedance to the 50-ohm coaxial feed line. A coaxial conical taper of 5.2 wavelengths was machined as an integral part of the slot piece and fulfilled the impedance-matching requirements. Nylon with $\epsilon_r = 3.02$ at 10 Gc served as the dielectric of the coaxial conical taper. The desired slot has a mean radius of 0.256-inch and 0.020-inch width. Slots of smaller width are practical but their impedance tends to zero and minimizes their efficiency as radiators. Figure 4 shows the schematic of the slot and tapering section with detailed machining dimensions. The rectangular slot was constructed using two waveguide sections as shown in Figure 5. Two brass pieces were machined and inserted in the guides, with the small dimension of the guide gradually taper-in to a 0.0312-inch slot.

Because of the inherent difficulties encountered in the measurement of the slot antenna admittance at the aperture itself, the VSWR and the shift of the null from the short circuit to the loaded condition were measured at the input of the tapered transition section. These two parameters were measured by means of a standard slotted-section technique for different simulated plasma thicknesses. The knowledge of the VSWR and the null shift permits the calculation of the slot admittance by using the Smith Chart or the well-known transmission line equation. The measured value of the admittance could be transferred to any point on the taper had the variation of the characteristic admittance with the taper length been known which is not the case for the linear taper used. A short-circuit test performed on the taper indicatesthat this structure has negligible losses and, consequently, it can be considered as an ideal transformer. Hence, the functional dependence of the layer thickness on the slot radiation admittance as measured at the input of the taper should be the same as it would be at the plane of the slot itself.

3.2 Results

The experimental antennas patterns are shown in Fig. 6 for the annular slot. Of importance to note is the occurrence of the radiation maxima near the theoretical critical angle, $\theta_c = 37^\circ$ and a low gain region near $\theta = 0^\circ$. This is entirely as predicted by the theory [Tyras, 1962] . Theoretical curves for $a = .353\ \lambda_o$ and for $a = 1.41\ \lambda_o$ have been plotted and are compared with the experimental values in Figs. 6a and 6b respectively. Figure 6c shows experimental curves for $a = .706\ \lambda_o$ and for $a = 1.06\ \lambda_o$. Very good agreement with theory is evident in Fig. 6a, but significant discrepancies are noted in Fig. 6b. As will be seen later, the same situation occurred in the case of the rectangular slot.

The results of the admittance measurements for the annular slot are seen in Fig. 7. Reference to theoretical curves [Galejs, 1964] shows that the experimental curves are of the same general shapes as those predicted. One notable discrepancy is seen in the curve for the normalized conductance. The theory predicts approximately a 5:1 ratio between the maximum and minimum values of G/Y_o, while the experimental curve shows approximately a 1.1:1 ratio.

The radiation patterns of the rectangular slot are seen in Fig. 8. Again, note the occurrence of radiation maxima near the predicted critical angle, $\theta_c = 37^o$. Theoretical curves for $a = .353\ \lambda$ and for $a = 1.41\ \lambda_o$ have been plotted and compared with the experimental values in Figs. 8a and 8b respectively. As observed previously, the pattern for the small sheath thickness of $.353\ \lambda_o$ agrees quite well with theory, while the same significant discrepancies are noted for the large thickness. Figure 8c shows experimental radiation patterns for sheath thicknesses of $.706\ \lambda_o$ and $1.06\ \lambda_o$.

In evaluating these results, it is well to keep in mind any approximations made in obtaining the theoretical radiation patterns. For the problem at hand, the method of saddle point integration has been used. This method allows the representation of an integral in the form of a series of inverse powers of distance from the source [Brekhovskikh, 1960] . It is assumed that a portion of the integrand, which in the present problem is the angular variation of the pattern, varies slowly. That is, its derivatives are sufficiently small so that the expansion may be limited to the first term. This approximation becomes better further from the source.

Now, reference to Fig. 8 shows that for large plasma thicknesses, the angular variation becomes quite rapid near the critical angle. In fact, one can show that at the critical angle, the first derivative is proportional

to the square of the layer thickness. The situation then, is the following. In the case of small plasma thicknesses, the slowly varying assumption is valid for the radial spacing between source and pickup available to the simulation technique. As the thickness increases, however, the angular variation near the critical angle becomes more rapid and the calculated results become less accurate. Physical limitations prevent the increase of radial spacing. Thus, to obtain better agreement with the simulated patterns, it becomes necessary to include a second term in the saddle point approximation. At present, however, the second term has not yet been evaluated and, consequently, the theoretical results include the contribution of the first term only.

Another major factor contribution to the discrepancies in the radiation patterns stems from the fact that the physical boundaries of the system are not sufficient to provide the minimum required far-field distance for thicknesses greater than 0.45 λ_o. The dependence of the minimum far-field distance on the sheath thickness is seen in Fig. 9. This curve was plotted by considering the half power bandwidth of the radiation pattern around the critical angle. The half power bandwidths were calculated from equation (11b). Now from Silver [1949] we have

$$\theta_{HPBW} \approx 60^{o} \left(\frac{\lambda}{d}\right)_{min} ,$$

which yields d/λ , and subsequently the minimum far-field distance. Thus the radiation pattern for $a = .353\ \lambda_o$ is well in the radiation field, while that for $a = 1.41\ \lambda_o$ is in the near field.

The admittance curves for the rectangular slot are seen in Fig. 10. Theoretical calculations have been made by Galejs [1964]. Comparison with these curves shows that the experimental curve for the normalized conductance agrees quite well with the theory. The same can be said for the normalized

susceptance curve except for very thin layers.

4. Conclusions

In the present work only the simplest case of the plasma sheath environment was treated, i.e., the case of a lossless, isotropic and homogeneous plasma. The simulation technique has been successfully tested only for this simplest case but it is clear that it may be used for the study of more complex plasma sheath models. The inherent simplicity of this experimental system and its versatility suggest that the method is capable of simulating more realistic plasma sheath environments which are not readily amenable to analytic solutions.

The most serious limitation of the present technique is the fact that the method is not capable of simulating plasmas characterized by a negative dielectric constant. Moreover, the effective simulated dielectric constant of 0.36 achieved with the Aroclor 1232 - air combination cannot be readily lowered because of the lack of suitable liquid dielectrics with $\epsilon_r > 2.8$. However, since the reentry communication systems can be expected to work well above the plasma frequency, the above limitations may not be serious ones indeed.

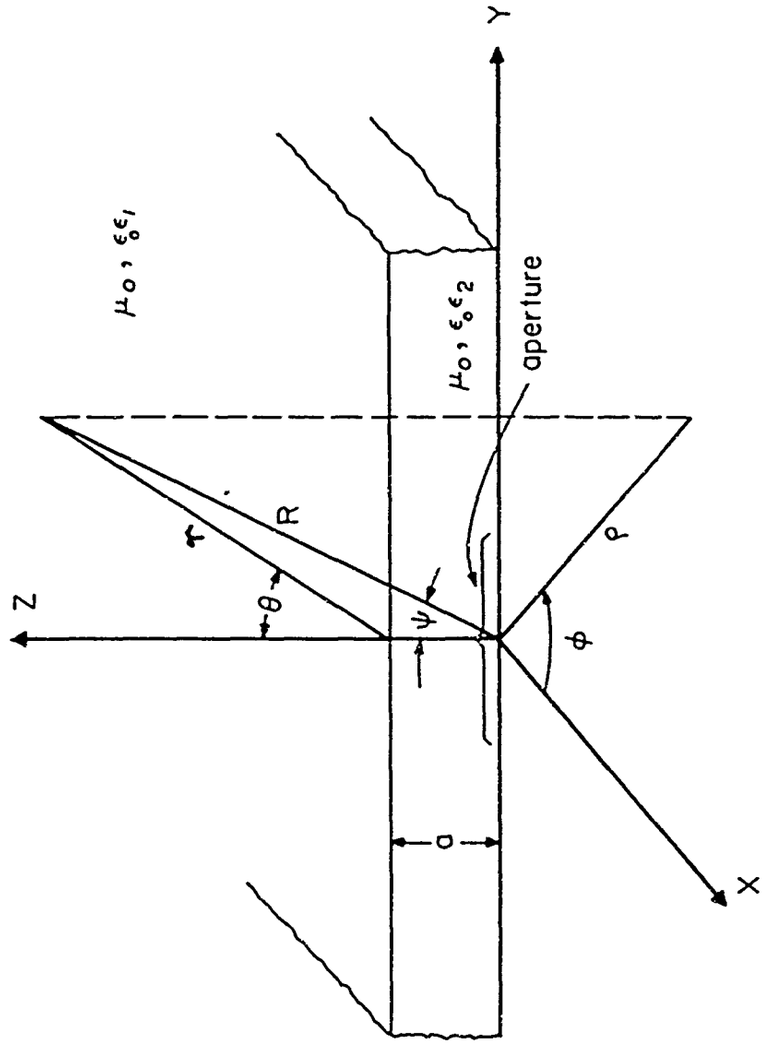

Fig. 1. Plasma Clad Slot Antenna Geometry

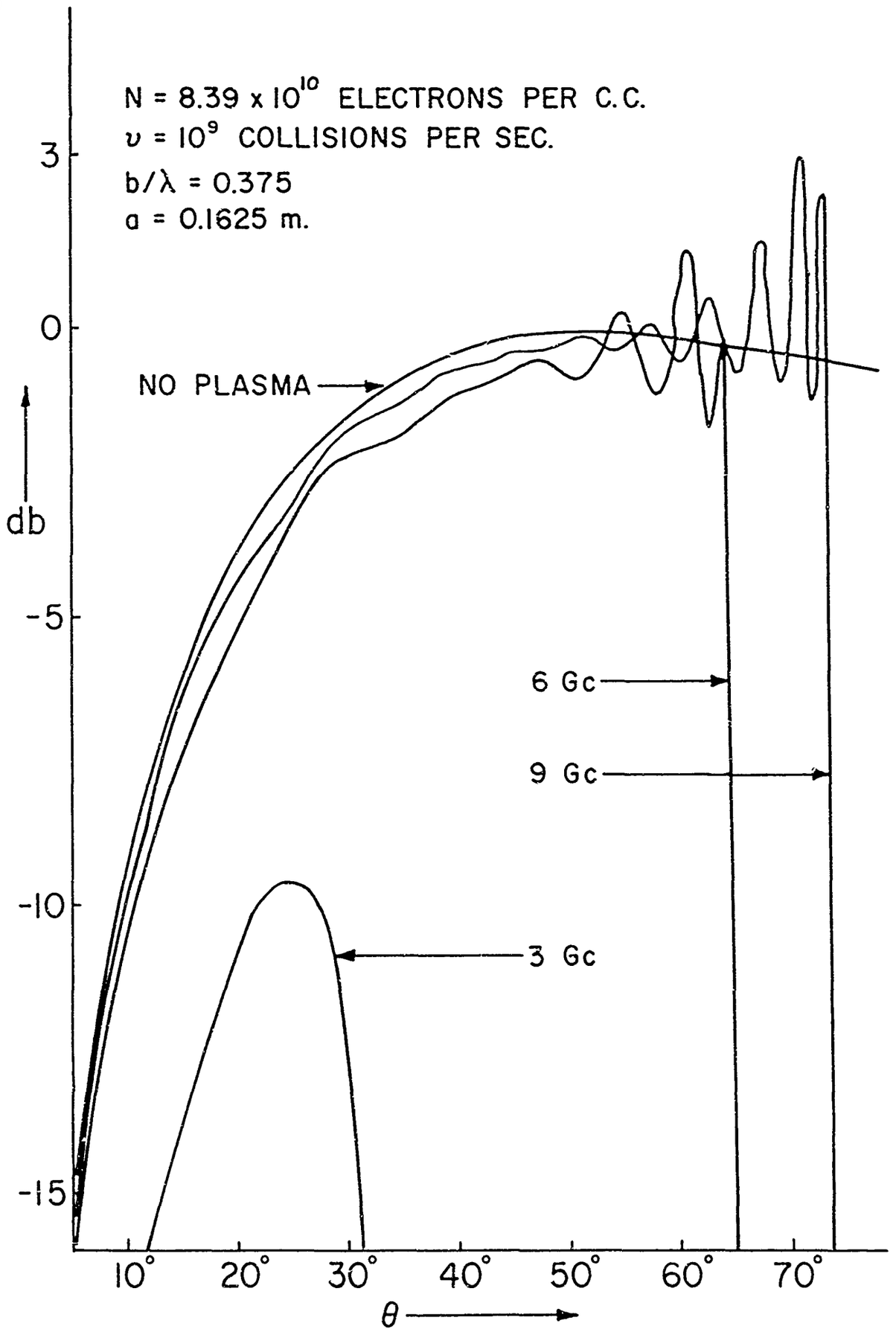

Fig. 2. Theoretical Radiation Patterns of a Plasma Clad Annular Slot

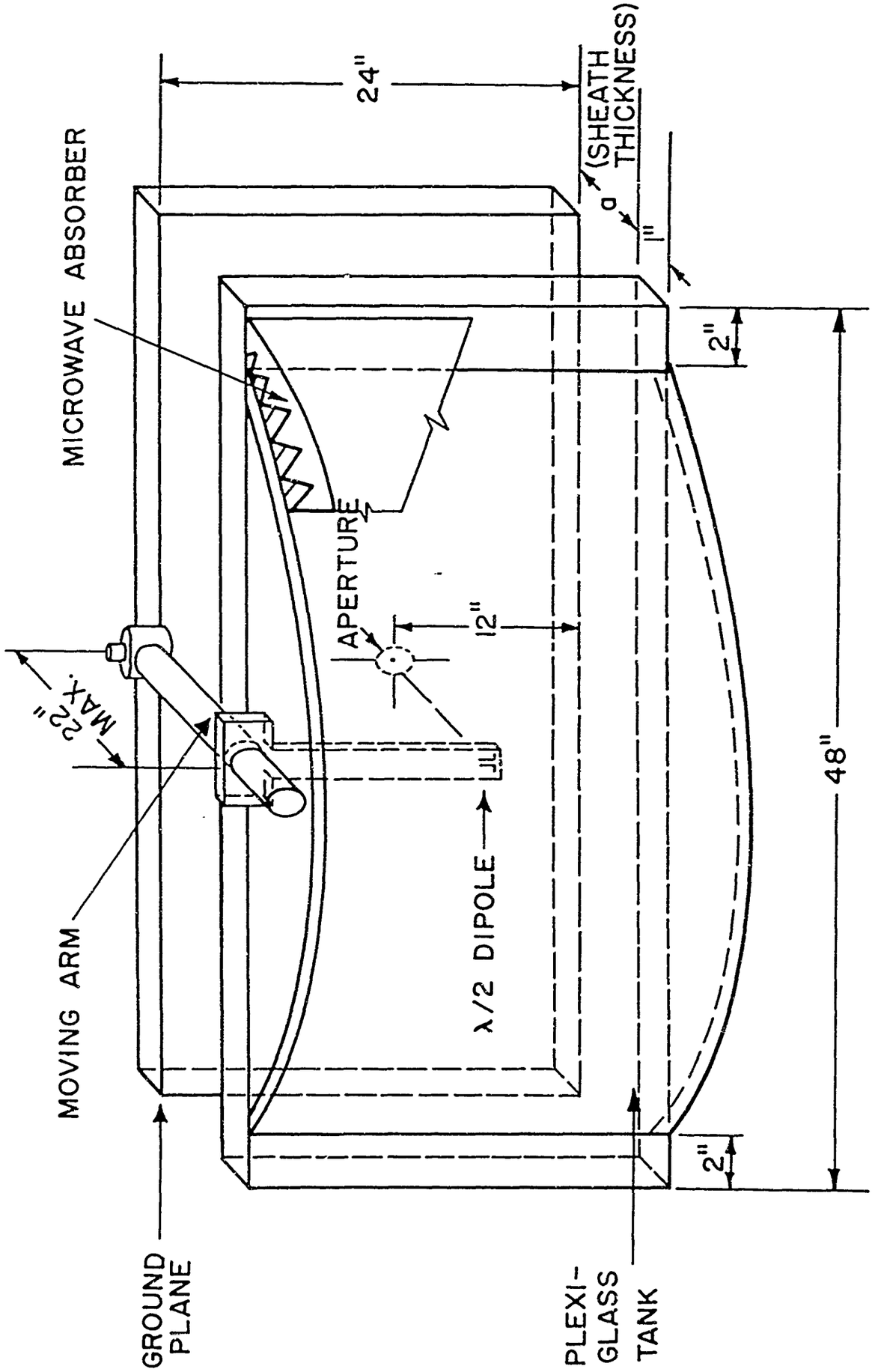

Fig. 3. The Simulation Tank

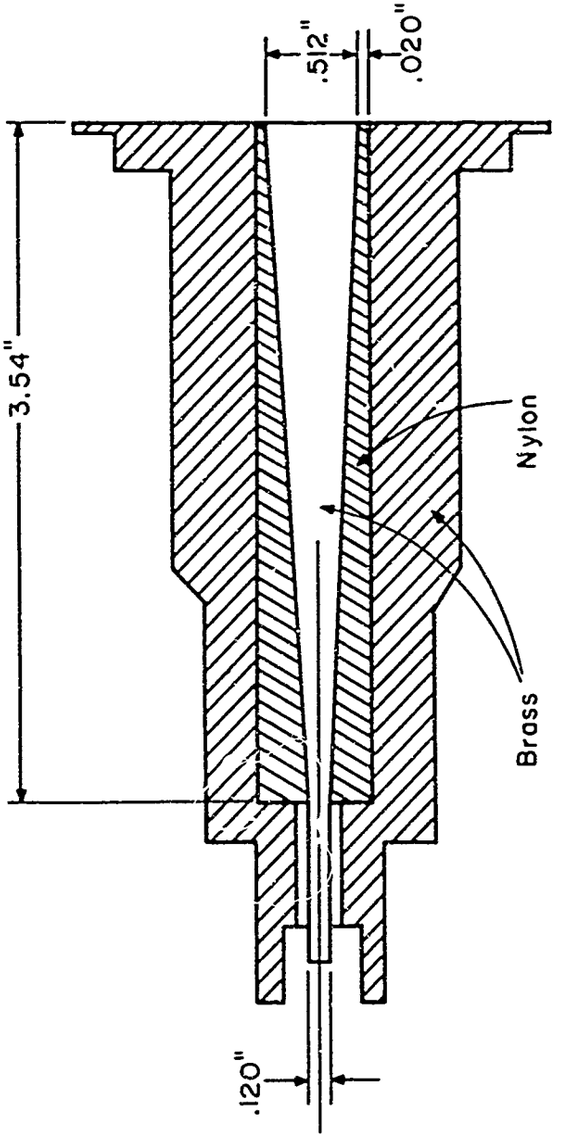

Fig. 4. Annular Slot Construction

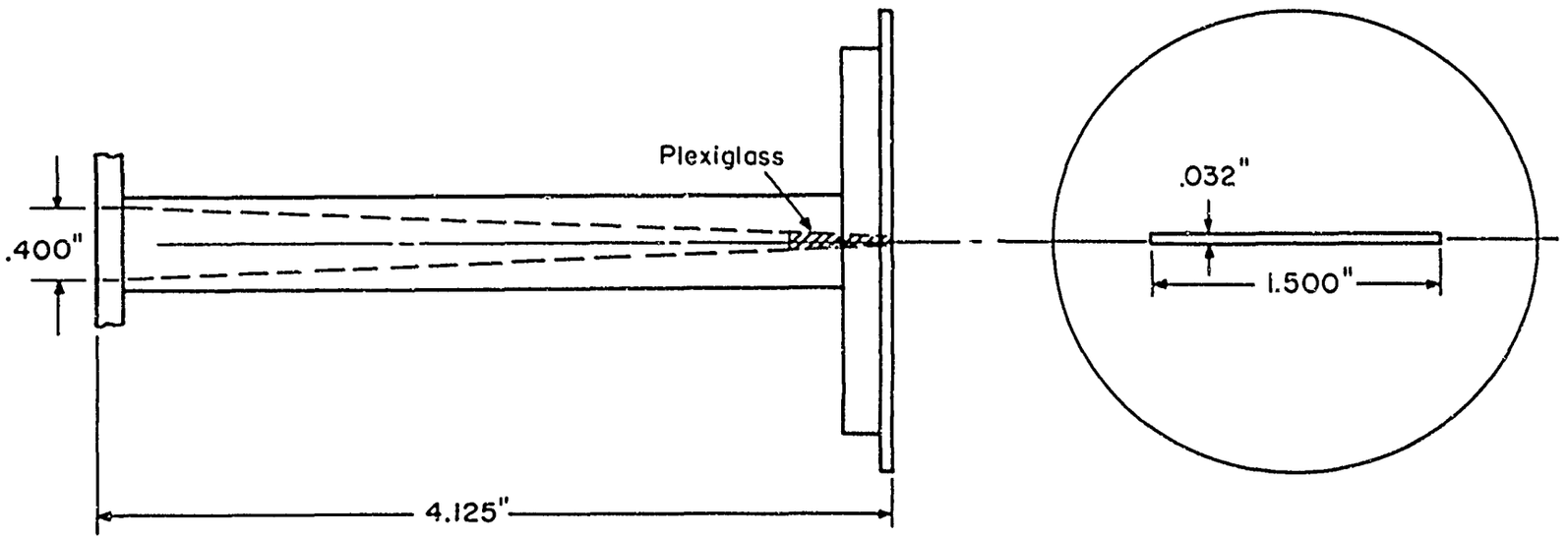

Fig. 5. Rectangular Slot Construction

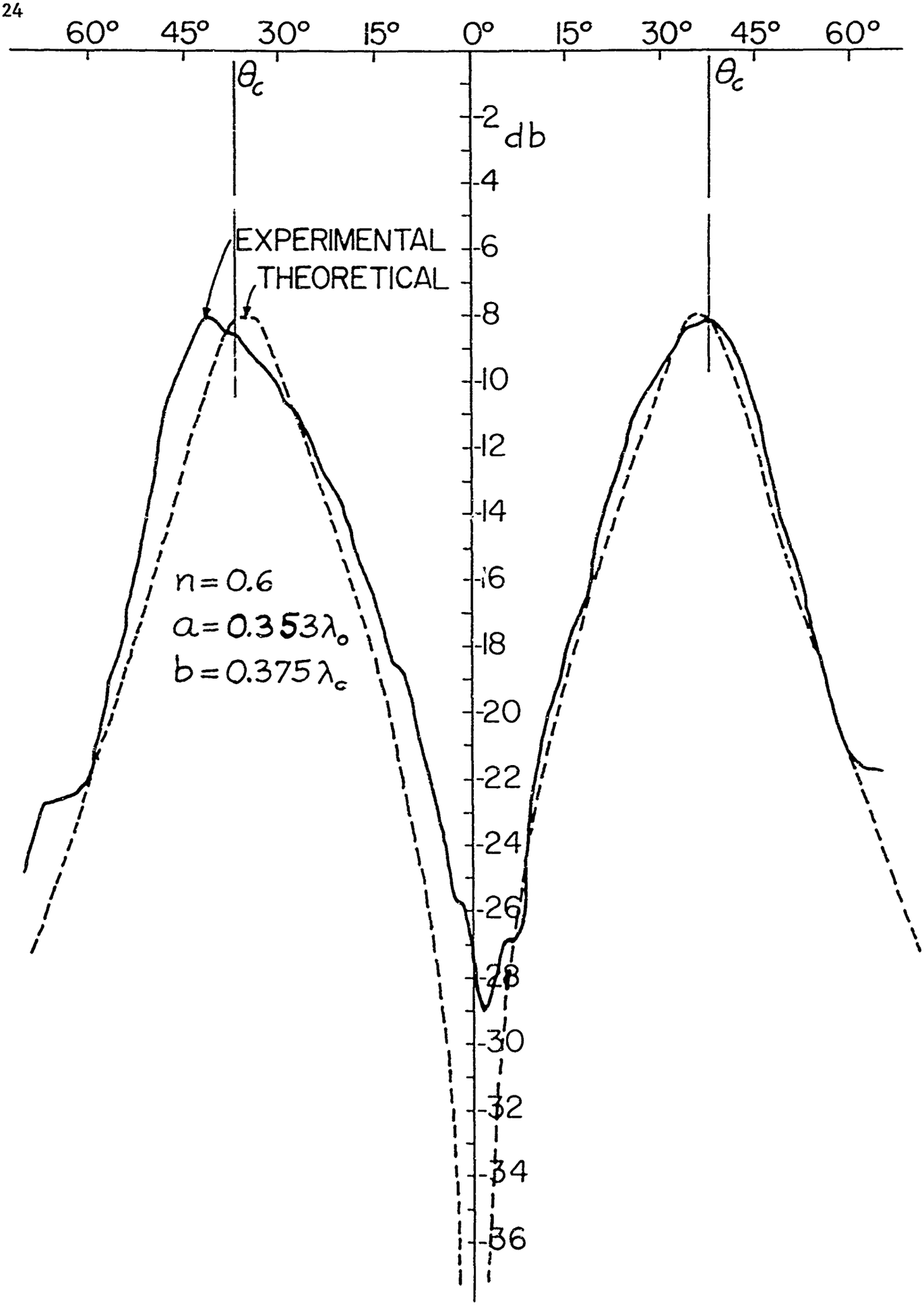

Fig. 6a. Experimental and Theoretical Radiation Patterns of the Plasma Clad Annular Slot

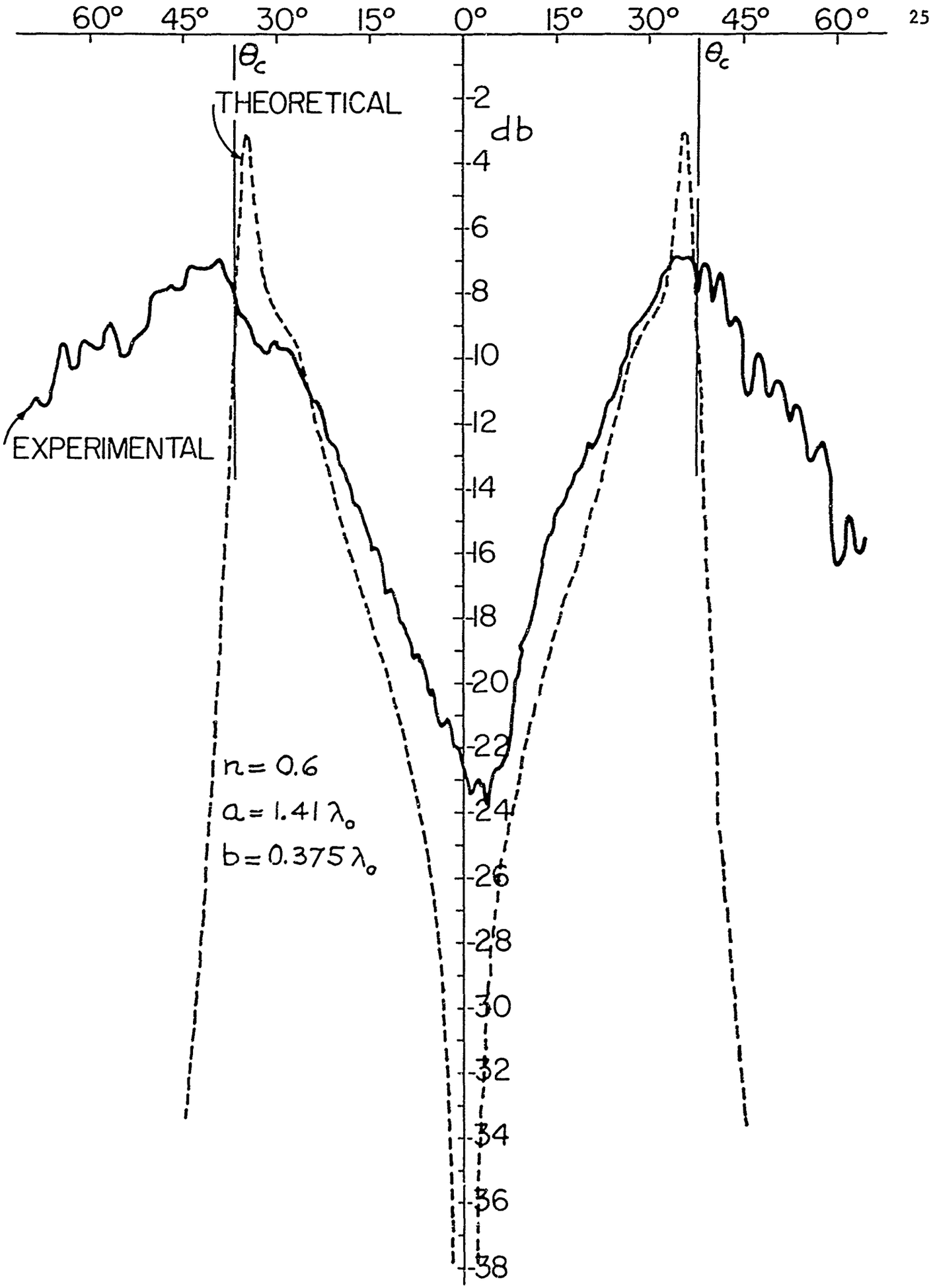

Fig. 6b. Experimental and Theoretical Radiation Patterns of the Plasma Clad Annular Slot

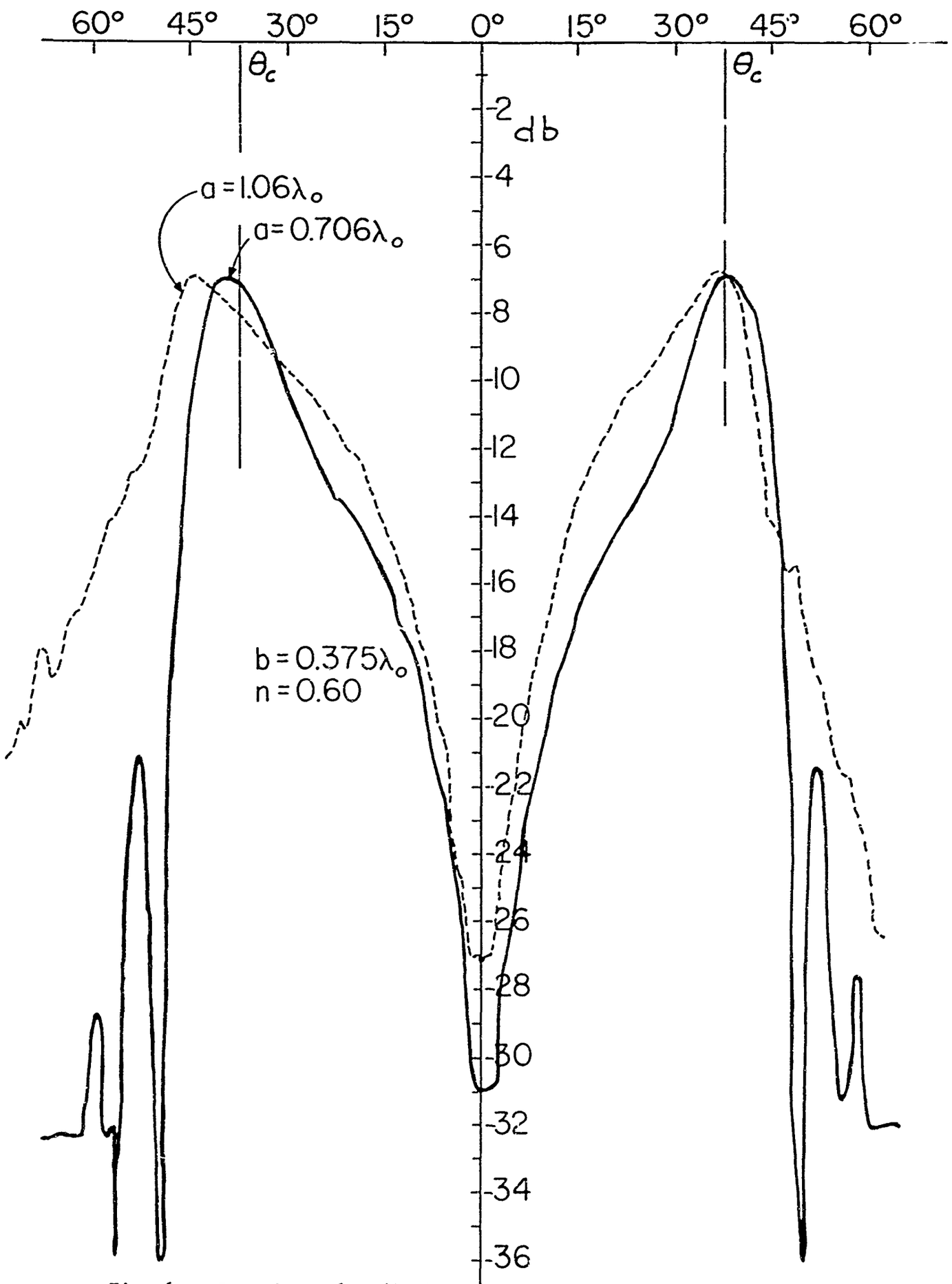

Fig. 6c. Experimental Radiation Patterns of the Plasma Clad Annular Slot

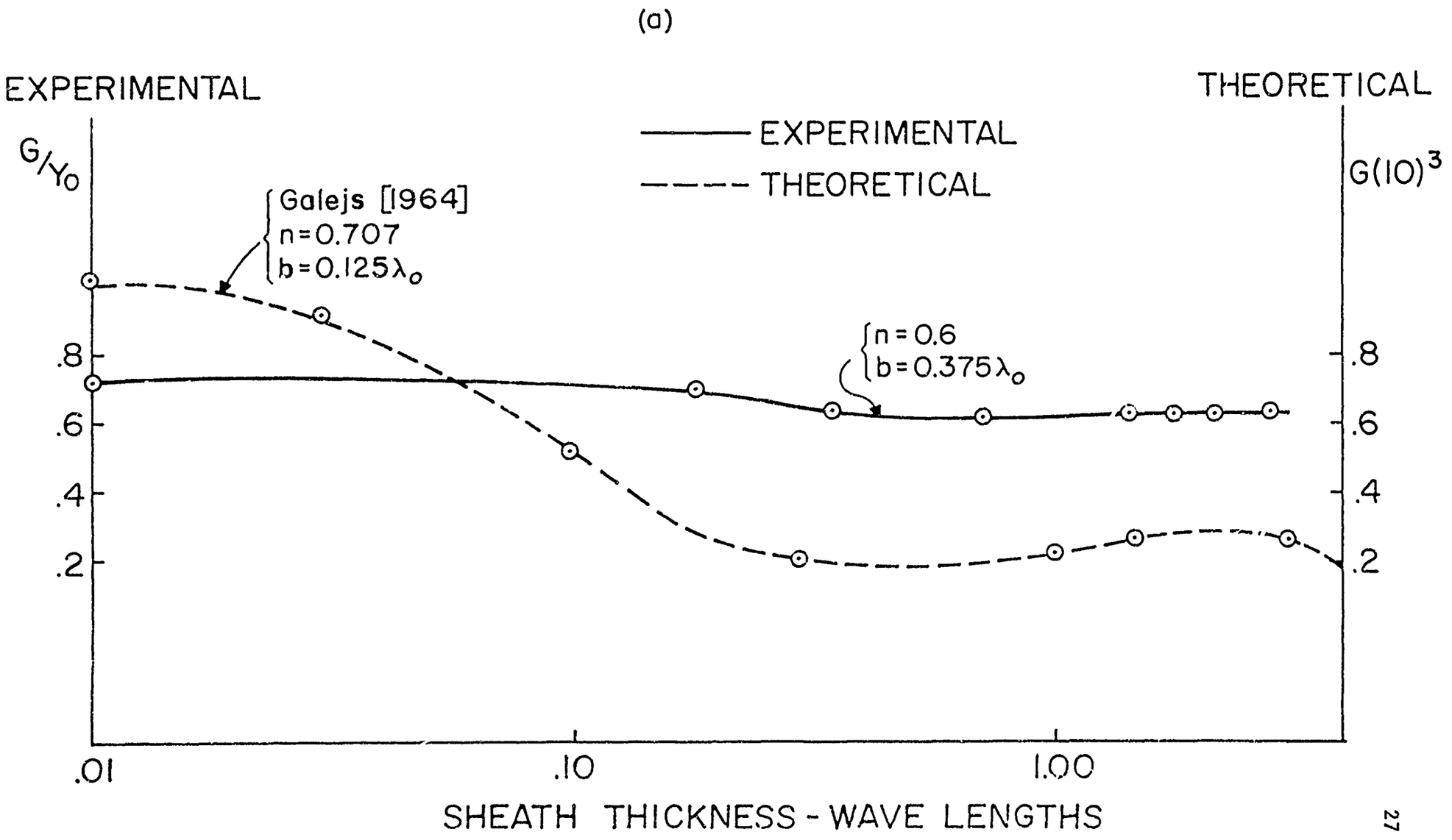

Fig. 7a. Admittance Characteristics of the Plasma Clad Annular Slot

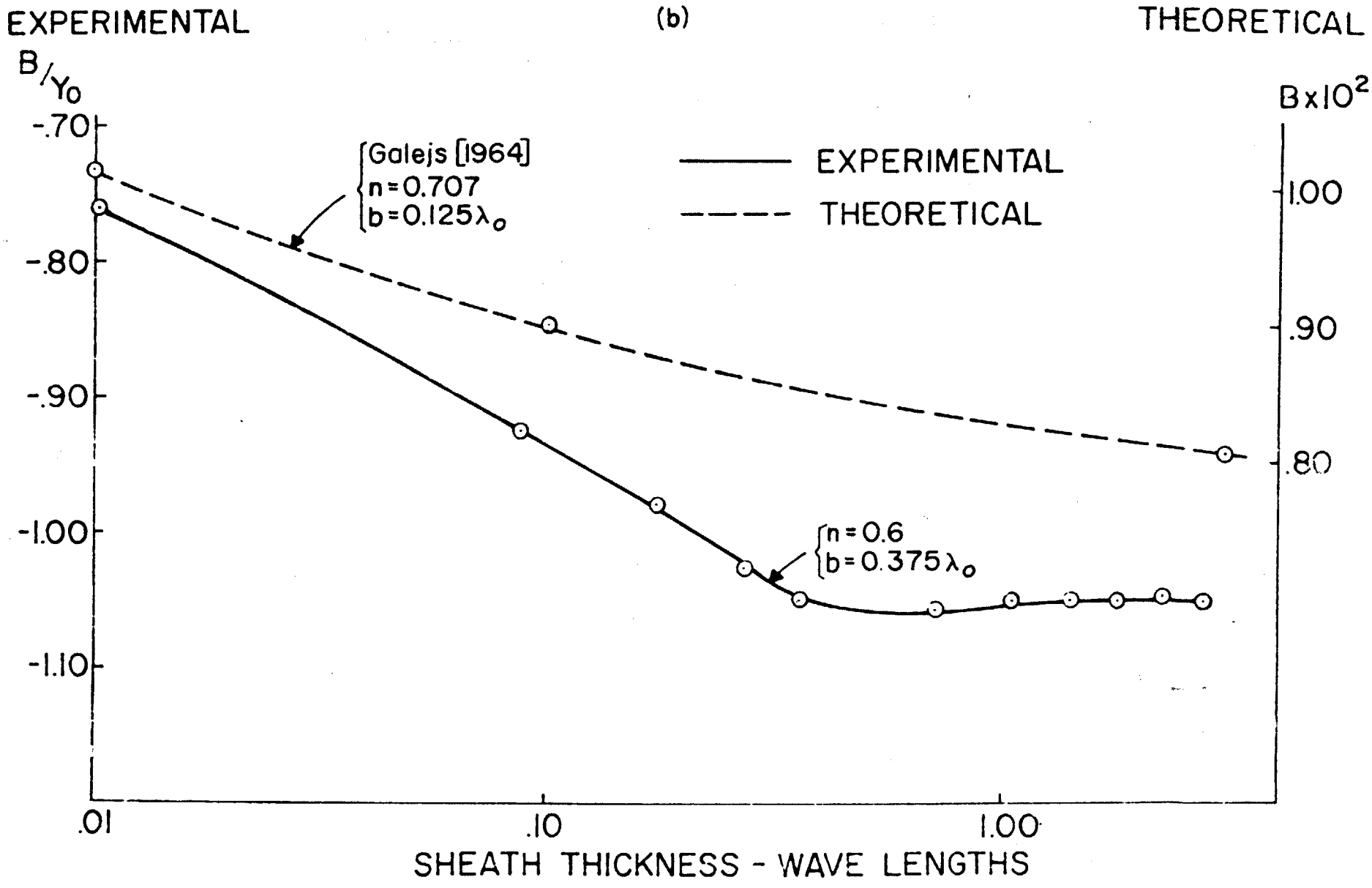

Fig. 7b. Admittance Characteristics of the Plasma Clad Annular Slot

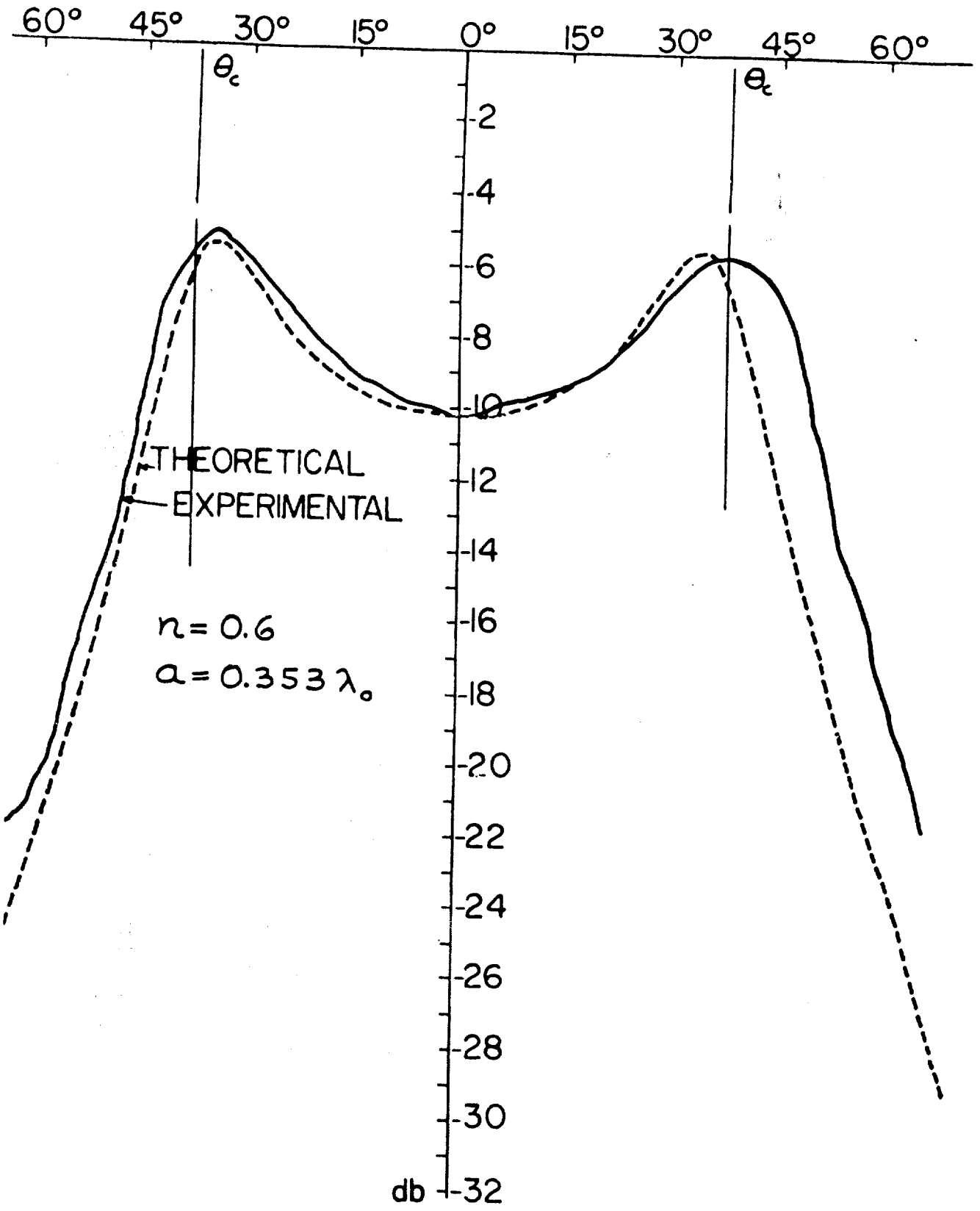

Fig. 8a. Experimental and Theoretical Radiation Patterns of the Plasma Clad Rectangular Slot

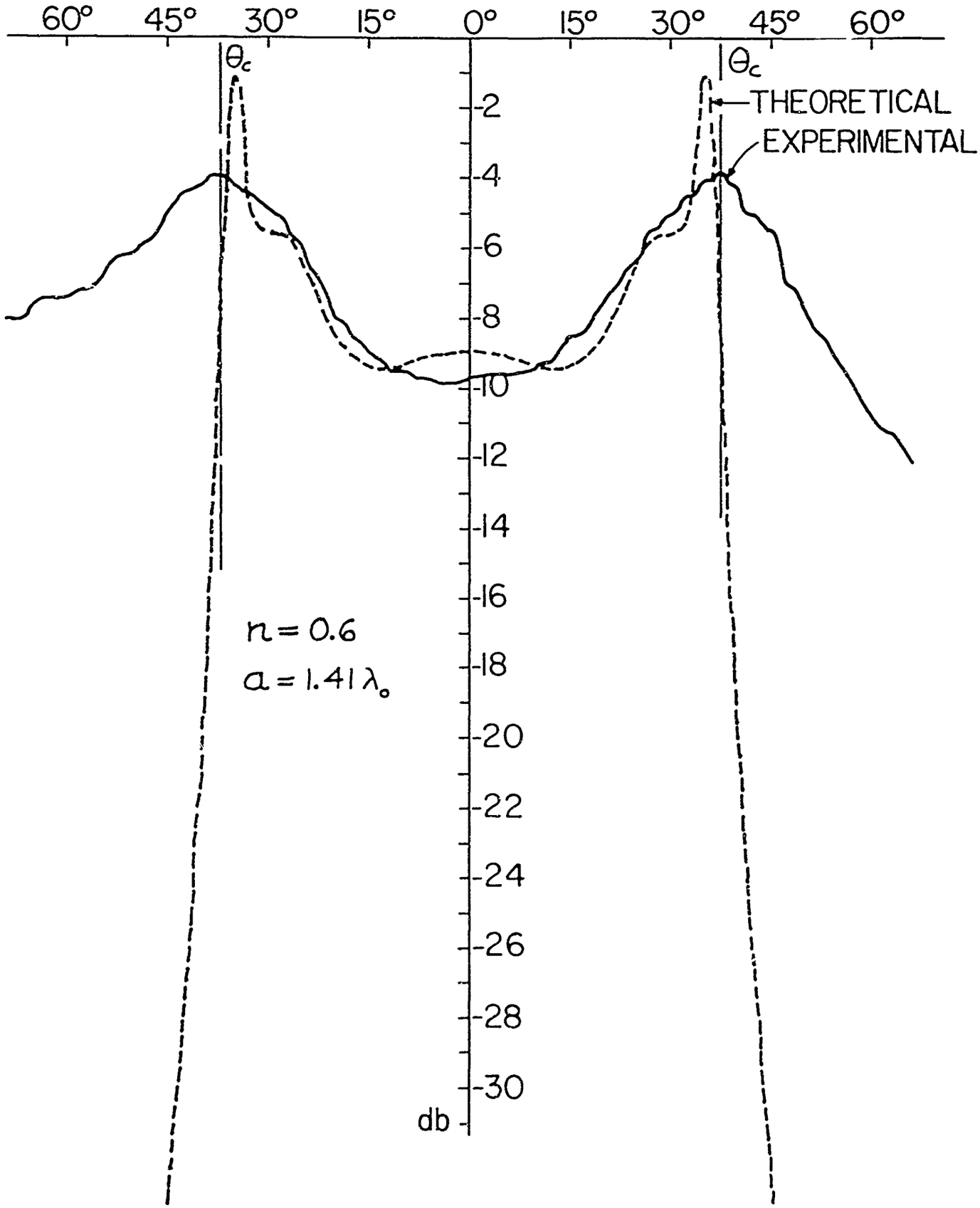

Fig. 8b. Experimental and Theoretical Radiation Patterns of the Plasma Clad Rectangular Slot

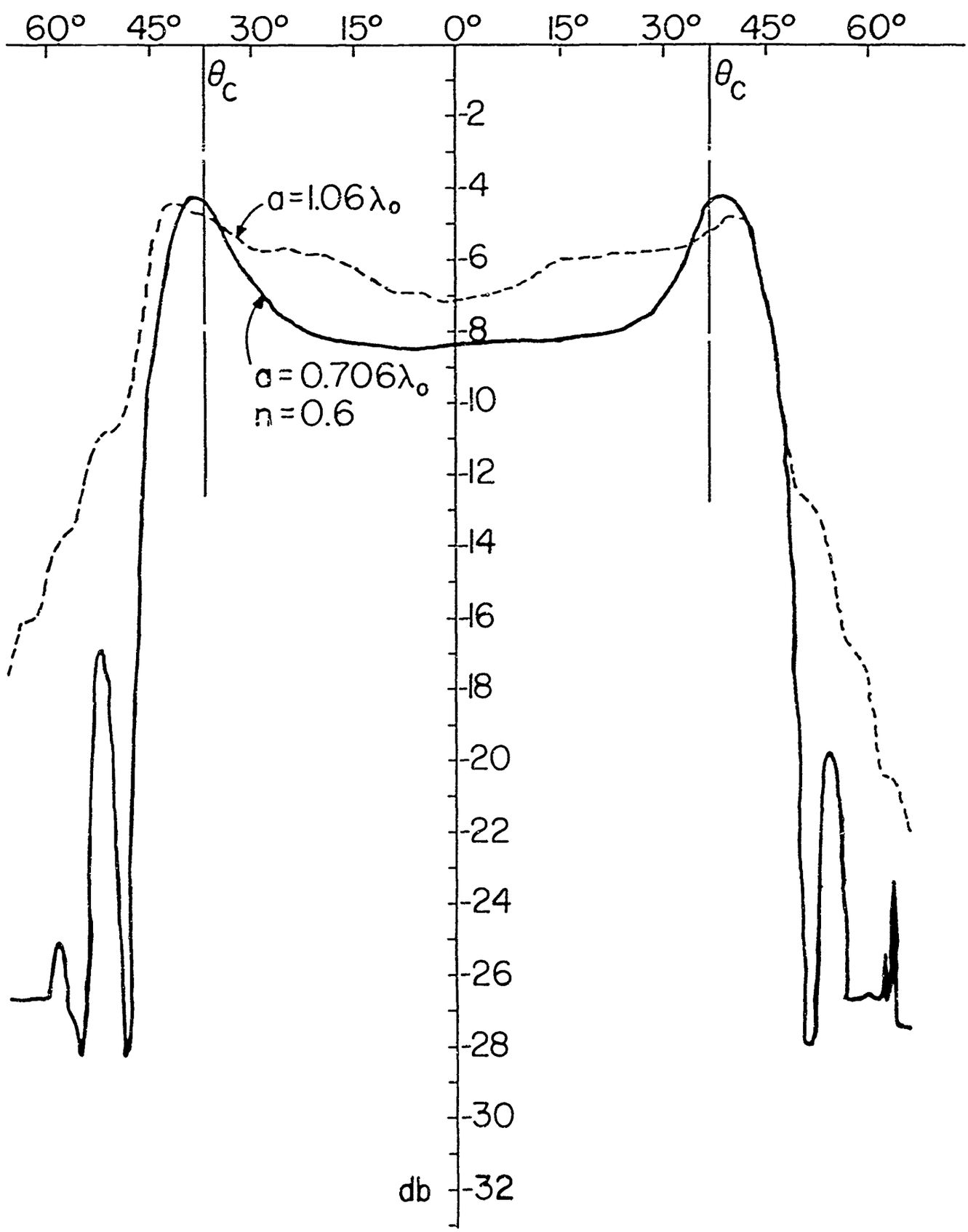

Fig. 8c. Experimental Radiation Patterns of the Plasma Clad Annular Slot

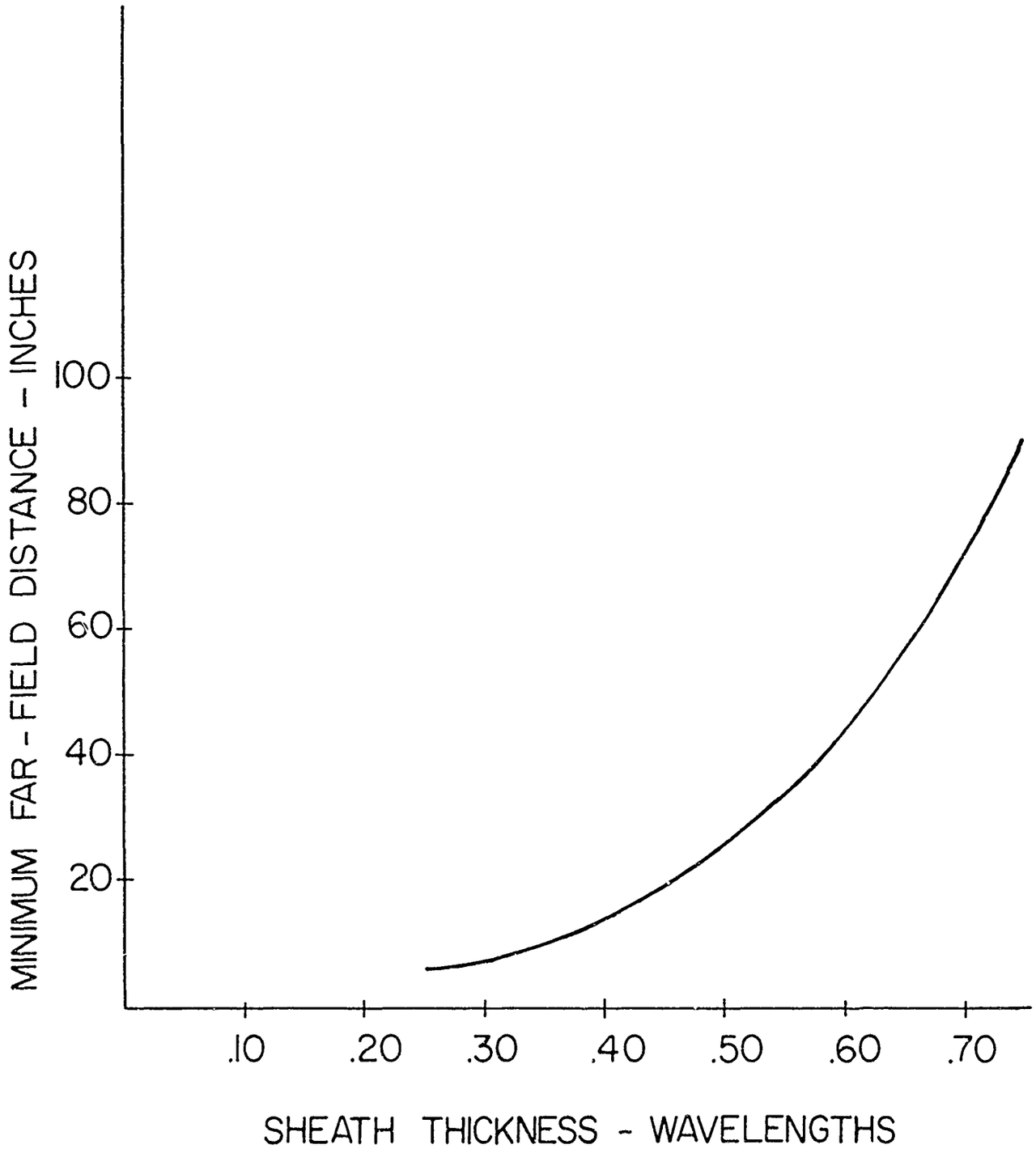

Fig. 9. Functional Dependence of the Minimum Far-Field Distance Versus Sheath Thickness

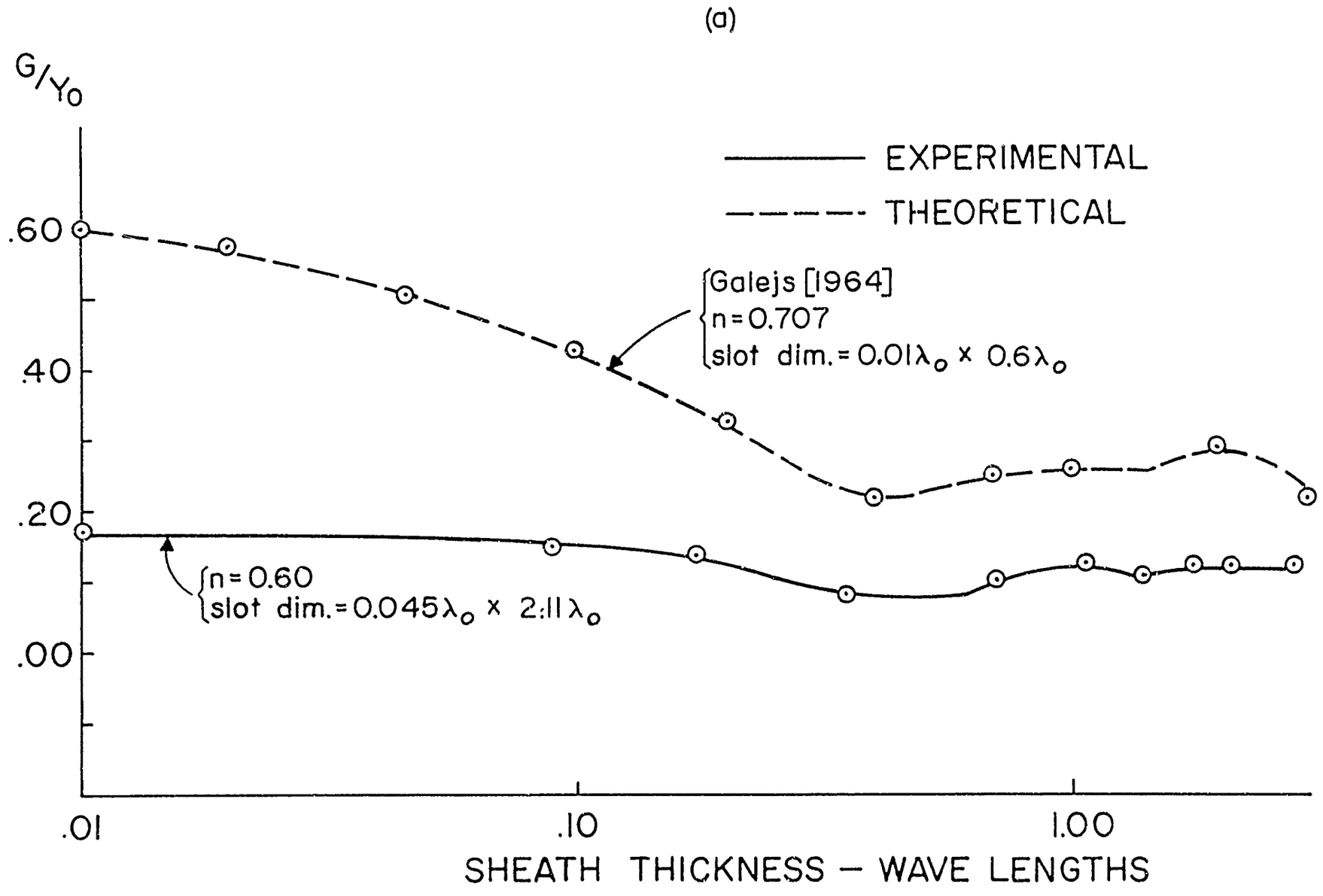

Fig. 10a. Admittance Characteristics of the Plasma Clad Rectangular Slot

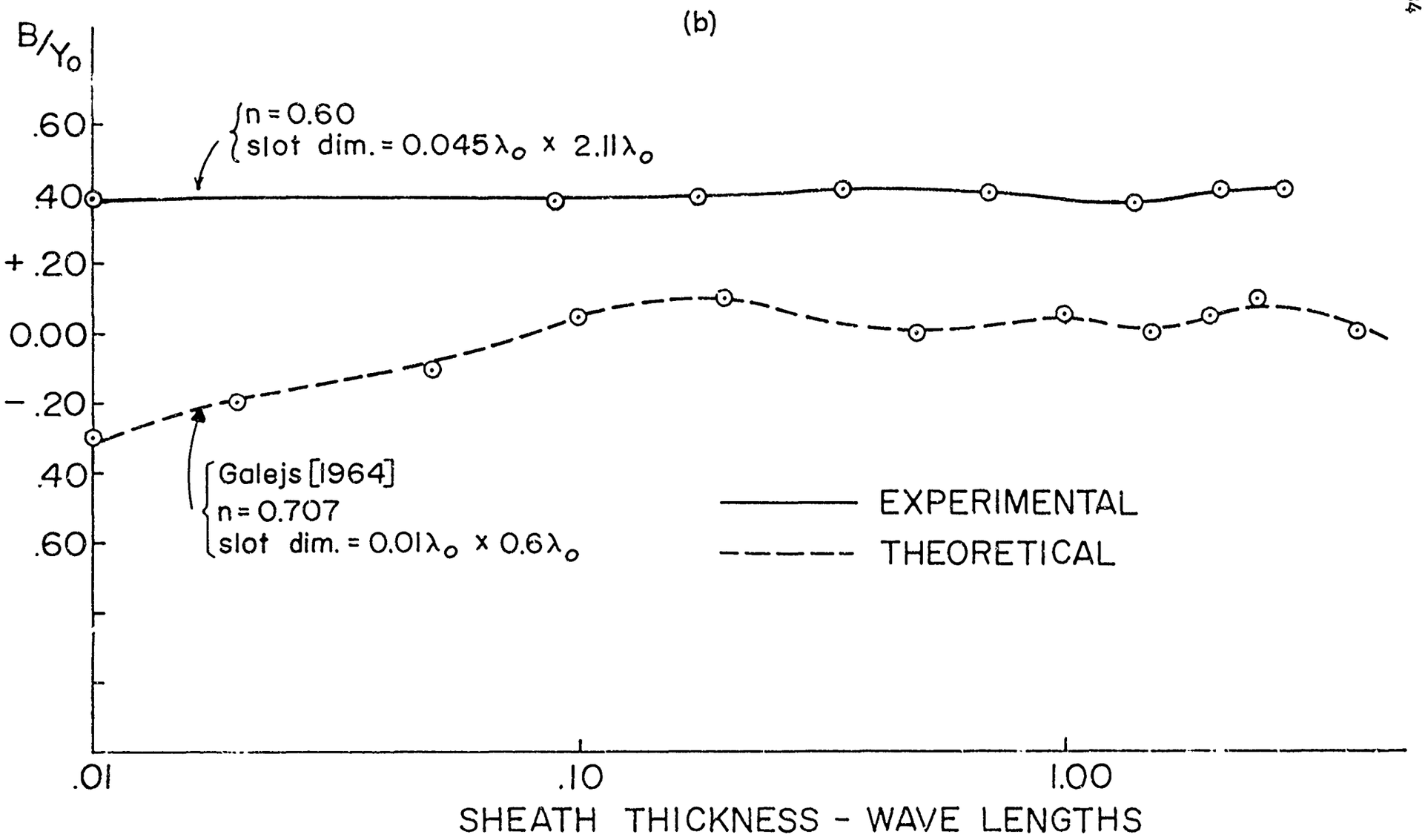

Fig. 10b. Admittance Characteristics of the Plasma Clad Rectangular Slot

5. References

Brekhovskikh, L. M. (1960), Waves in layered media, Vol. 6, 245-250 (Academic Press Inc., New York).

Brown, M. A. (May, 1953), Artificial dielectrics having refractive indices less than unity, Proc. IEE, Monograph No. 62R, Vol. 100, part 4, 51-62.

Galejs, J. (January, 1964), Admittance of a waveguide radiating into a stratified plasma, Research Report No. 347R, Applied Res. Lab., Sylvania Electronic Systems.

Galejs, J. (March, 1964), Admittance of annular slot antennas radiating into a plasma layer, Radio Sci. J. Res. NBS/USNC-URSI, No. 3, 317-324.

Golden, K. E. (May, 1964), A study of artificial dielectrics, Plasma Res. Lab., Aerospace Corp., Contract No. AF 04(695)-269.

Golden, K. E., and T. M. Smith, (March, 1964), Simulation of a thin plasma sheath by a plane of wires, Plasma Res. Lab., Aerospace Corp., Contract No. AF 04(695)-269.

Knop, C. M., and G. I. Cohn, (April, 1964), Radiation from an aperture in a coated plane, Radio Sci. J. Res. NBS/USNC-URSI 68D, No. 4, 363-378.

Newstein, M., and J. Lurye, (July, 1956), The field of a magnetic line source in the presence of a layer of complex refractive index, Technical Res. Group, Sci. Report No. 1, New York.

Omura, M. (December, 1962), Radiation pattern of a slit in a ground plane covered by a plasma layer, Air Force Cambridge Res. Lab., AFCRL-62-958.

Rotman, W. (January, 1962), Plasma simulation by artificial dielectric and parallel-plate media, IRE Trans. on Antennas and Propagation, Vol. AP-10, No. 1, 82-95.

Silver, S. (1949), Microwave Antenna Theory and Design, (McGraw-Hill, New York).

Stratton, J. A. (1941), Electromagnetic Theory, 488-489, (McGraw-Hill, New York).

Tamir, T., and A. A. Oliner, (January, 1962), The influence of complex waves on the radiation field of a slot-excited plasma layer, IRE Trans. on Antennas and Propagation, Vol. AP-10, No. 1, 55-65.

Tyras, G. (1962), Field of an annular slot covered with plasma, The Boeing Company, Doc. No. D2-80411.

Von Hippel, A. R. (1958), Dielectric materials and applications, 300-370 (John Wiley and Sons, New York).

Unclassified

Security Classification

DOCUMENT CONTROL DATA - R&D

(Security classification of title, body of abstract and indexing annotation must be entered when the overall report is classified)

1. ORIGINATING ACTIVITY *(Corporate author)*	2a. REPORT SECURITY CLASSIFICATION
Engineering Research Laboratories The University of Arizona Tucson, Arizona	Unclassified
	2b. GROUP

3. REPORT TITLE

AN EXPERIMENTAL STUDY OF PLASMA SHEATH EFFECTS ON ANTENNAS

4. DESCRIPTIVE NOTES *(Type of report and inclusive dates)*

Final report Dec. 1963-Dec. 1964

5. AUTHOR(S) *(Last name, first name, initial)*

Tyras, George; Bargeliotes, Peter C., Hamm, John M., and Schell, Robert R.

6. REPORT DATE	7a. TOTAL NO. OF PAGES	7b. NO. OF REFS
December 1964	40	15

8a. CONTRACT OR GRANT NO.	9a. ORIGINATOR'S REPORT NUMBER(S)
AF19(628)-3834	
b. PROJECT NO. 4642	1
c. TASK 464202	9b. OTHER REPORT NO(S) *(Any other numbers that may be assigned this report)*
d.	AFCRL-65-53

10. AVAILABILITY/LIMITATION NOTICES

Qualified requesters may obtain copies of this report from DDC.

11. SUPPLEMENTARY NOTES	12. SPONSORING MILITARY ACTIVITY
Simulation of Plasma Sheath	Air Force Cambridge Research Laboratories, Office of Aerospace Research, USAF, Bedford, Mass.

13. ABSTRACT

A plasma simulation technique has been developed which can be used to study the effects of homogeneous or inhomogeneous plasma sheaths on the radiation pattern deterioration and input impedance of microwave antennas. A tank has been designed and constructed for use in the simulation technique which can reproduce by means of real dielectric materials the dielectric constant encountered in plasma covered antenna research. (U)

The radiation patterns and input impedances of an annular slot and a thin and long rectangular slot have been successfully measured in the presence of a simulated loss-less, homogeneous, and isotropic plasma layer of varied thickness. Comparison with the theoretical data indicates a generally good agreement, although some differences exist. In the case of the radiation patterns these differences are attributed to the finite distance between the radiator and the receiving antenna on the one hand and the inherent inaccuracy of the saddle point method of integration in certain regions on the other hand. (U)

DD FORM 1 JAN 64 1473

Unclassified

Security Classification

14. KEY WORDS	LINK A		LINK B		LINK C	
	ROLE	WT	ROLE	WT	ROLE	WT
Plasma simulation technique	8	3				
Plasma sheath	6	2				
Radiation pattern deterioration	7	2				
Input impedance	7	2				
Tank	5	1				
Real dielectric materials	9	2				
Dielectric constant	8	2				
Slot antenna			5	1		
Simulated plasma			8	2		
Varied thicknesses			5	2		
Theoretical comparison			2	2		

INSTRUCTIONS

1. ORIGINATING ACTIVITY. Enter the name and address of the contractor, subcontractor, grantee, Department of Defense activity or other organization *(corporate author)* issuing the report.

2a. REPORT SECURITY CLASSIFICATION: Enter the overall security classification of the report. Indicate whether "Restricted Data" is included. Marking is to be in accordance with appropriate security regulations.

2b. GROUP: Automatic downgrading is specified in DoD Directive 5200.10 and Armed Forces Industrial Manual. Enter the group number. Also, when applicable, show that optional markings have been used for Group 3 and Group 4 as authorized.

3. REPORT TITLE: Enter the complete report title in all capital letters. Titles in all cases should be unclassified. If a meaningful title cannot be selected without classification, show title classification in all capitals in parenthesis immediately following the title.

4. DESCRIPTIVE NOTES: If appropriate, enter the type of report, e.g., interim, progress, summary, annual, or final. Give the inclusive dates when a specific reporting period is covered.

5. AUTHOR(S): Enter the name(s) of author(s) as shown on or in the report. Enter last name, first name, middle initial. If military, show rank and branch of service. The name of the principal author is an absolute minimum requirement.

6. REPORT DATE. Enter the date of the report as day, month, year, or month, year. If more than one date appears on the report, use date of publication.

7a. TOTAL NUMBER OF PAGES: The total page count should follow normal pagination procedures, i.e., enter the number of pages containing information.

7b. NUMBER OF REFERENCES: Enter the total number of references cited in the report.

8a. CONTRACT OR GRANT NUMBER. If appropriate, enter the applicable number of the contract or grant under which the report was written.

8b, 8c, & 8d. PROJECT NUMBER: Enter the appropriate military department identification, such as project number, subproject number, system numbers, task number, etc.

9a. ORIGINATOR'S REPORT NUMBER(S): Enter the official report number by which the document will be identified and controlled by the originating activity. This number must be unique to this report.

9b. OTHER REPORT NUMBER(S): If the report has been assigned any other report numbers *(either by the originator or by the sponsor)*, also enter this number(s).

10. AVAILABILITY/LIMITATION NOTICES: Enter any limitations on further dissemination of the report, other than those imposed by security classification, using standard statements such as:

(1) "Qualified requesters may obtain copies of this report from DDC."

(2) "Foreign announcement and dissemination of this report by DDC is not authorized."

(3) "U. S. Government agencies may obtain copies of this report directly from DDC. Other qualified DDC users shall request through

_____."

(4) "U. S. military agencies may obtain copies of this report directly from DDC. Other qualified users shall request through

_____."

(5) "All distribution of this report is controlled. Qualified DDC users shall request through

_____."

If the report has been furnished to the Office of Technical Services, Department of Commerce, for sale to the public, indicate this fact and enter the price, if known.

11. SUPPLEMENTARY NOTES: Use for additional explanatory notes.

12. SPONSORING MILITARY ACTIVITY: Enter the name of the departmental project office or laboratory sponsoring *(paying for)* the research and development. Include address.

13. ABSTRACT: Enter an abstract giving a brief and factual summary of the document indicative of the report, even though it may also appear elsewhere in the body of the technical report. If additional space is required, a continuation sheet shall be attached.

It is highly desirable that the abstract of classified reports be unclassified. Each paragraph of the abstract shall end with an indication of the military security classification of the information in the paragraph, represented as *(TS), (S), (C), or (U).*

There is no limitation on the length of the abstract. However, the suggested length is from 150 to 225 words.

14. KEY WORDS: Key words are technically meaningful terms or short phrases that characterize a report and may be used as index entries for cataloging the report. Key words must be selected so that no security classification is required. Identifiers, such as equipment model designation, trade name, military project code name, geographic location, may be used as key words but will be followed by an indication of technical context. The assignment of links, rules, and weights is optional.